distances from the nozzle, while Fig. 2 also shows $\sigma(y)$ calculated [5] for x = 40h. The discrepancies between theory and experiment are due to the calculations not incorporating the gradients in the averaged dielectric constant, inexact approximation for the kinetic-energy dissipation over the jet cross section, and the temperature-fluctuation dissipation, as well as the approximation involved in considering the jets similar.

The schlieren method can be applied to the scattered electromagnetic-radiation pattern and optical-parameter distributions in a shear-type turbulent flow. The known distribution for the scattering indicatrix enables one to recover the density-fluctuation spectrum [5]. Under certain conditions, the method can also be used to examine turbulence in temperature, concentration, and other patterns directly related to the density fluctuations.

NOTATION

$\langle I \rangle$, averaged radiation intensity; $\gamma(\omega \cdot \omega')$ scattering indicatrix as a function of the cosine of the scattering angle θ; $(\omega \cdot \omega') = \cos\theta$; Ω, surface of unit sphere; s, photographic sensitivity; Δt, exposure time; h, nozzle end thickness.

LITERATURE CITED

1. A. P. Ivanov, Scattering-Medium Optics [in Russian], Minsk (1969).
2. O. G. Martynenko and I. A. Vatutin, Izv. Akad. Nauk BSSR, Ser. Fiz.-Énerg. Nauk, No. 3, 41-45 (1987).
3. L. A. Vasil'ev, Schlieren Methods [in Russian], Moscow (1968).
4. Y. Bashir and M. S. Uberoi, Phys. Fluids, 18, No. 4, 405-410 (1975).
5. O. G. Martynenko, I. A. Vatutin, N. I. Lemesh, and P. P. Khramtsov, Inzh.-Fiz. Zh., 56, No. 1, 26-28 (1989).

LAWS GOVERNING THE INTERNAL REGION OF A TURBULENT BOUNDARY LAYER

V. V. Zyabrikov

UDC 532.526

A study was made of the effect of large positive pressure gradients on the distribution of friction and the velocity profile in the viscous sublayer, transitional section, and core of the internal region of a turbulent boundary layer.

The subdivision of an entire turbulent boundary layer into two regions — an internal region (the "wall" region) and an external region (the wake region) — is generally accepted in boundary layer theory [1-3] and reflects the fact, discovered by Clausius, that an external region where eddy viscosity can be assumed constant over the cross section exists a substantial distance from the wall. Eddy viscosity in this region decreases with approach toward the external boundary of the boundary layer due to alteration. In contrast to the external region, in the internal region the wall's effect on the size of the turbulent "eddies" causes eddy viscosity to decrease with decreasing distance to the wall. The flow characteristics in the internal region, with small-scale turbulence, depend only slightly on the history of the flow and are determined by the distance to the wall, the pressure gradient, and other local parameters [1, 2, 4]. It is known that pressure obeys the "wall law" in the internal region of turbulent boundary layers with small pressure gradients. This law, using dimensionless variables

$$\eta_* = \frac{yv_*}{\nu}, \quad u_* = \frac{u}{v_*} \quad \left(v_* = \sqrt{\frac{\tau_\omega}{\rho}}\right) \tag{1}$$

M. I. Kalinina Leningrad Polytechnic Institute.

Translated from Inzhenerno-Fizicheskii Zhurnal, Vol. 56, No. 5, pp. 719-725, May, 1989. Original article submitted December 2, 1987.

describes a single velocity profile with a linear section in the immediate vicinity of the wall and a logarithmic section at a certain distance from it [1, 2]. The profile is independent of the Reynolds number and the pressure gradient. Despite numerous studies, investigators have yet to determine the effect of moderate and large pressure gradients on a turbulent boundary layer in sections close to separation. Researchers have recently published very important results from direct measurements of a boundary layer with separation [4, 5] performed simultaneously by hot-wire and laser methods. These results are more accurate than data that has been published previously. The studies [4-6] represent valuable experimental material which made it possible to extend the approach proposed in [7] for study of the transitional section of a turbulent boundary layer to the case of a large pressure gradient. In contrast to [7], here we study the entire internal region, including the turbulent core. Under these conditions, the approximate binomial formula adopted in [7] for the shear stress distribution across the boundary layer – which ignores the effect of the inertial term – is no longer valid and is replaced by the more exact trinomial formula of Cowles [8]

$$\tau_* = 1 + p_*\eta_* + g_* \int_0^{\eta_*} u_*^2 \, d\eta_*. \tag{2}$$

Here, $\tau_* = \tau/\tau_w$, $p_* = (\nu/\rho)\,(dp/dx)/v_*^3$ is the pressure gradient parameter. The parameter $g_* = \nu(dv_*/dx)/v_*^2$ will be referred to as the convective acceleration parameter. As shown by simple calculations performed on the basis of experimental data on a gradientless boundary layer ($dp/dx = 0$) [1], an increase in the local Reynolds number R^{**} from 10^3 to 10^6 is accompanied by a reduction in the convective acceleration parameter g_* from 10^{-6} to 10^{-9}, i.e., this is a very small quantity. However, the integral next to g_* in Eq. (2) increases sharply with an increase in η_* (see the table in [8]), so that we can no longer ignore their product in the turbulent core. This also applies to the case $dp/dx \neq 0$. The experimental data in [9] confirm the need for such a refinement: even in the case of a gradientless boundary layer, the shear stress decreases by 10% at a distance from the wall corresponding to the thickness of the internal region. Thus, the assumption of a constant turbulent shear stress $\tau = \tau_w$ is invalid. This assumption was the basis for derivation of the logarithmic velocity profile

$$u_* = \frac{1}{\varkappa_*} \ln \eta_* + B_*. \tag{3}$$

Nevertheless, the logarithmic law has been confirmed by numerous experiments [10], not only for a plate, but also in the presence of a pressure gradient. The latter is possible only in the case when the pressure gradient, influencing the turbulent shear stress distribution [see Eq. (2)], also determines the distribution of the mixing length. These changes offset one another. As was shown in [11], the logarithmic section is more conservative in regard to a change in the pressure gradient than is the linear formula for mixing length. The retention of the slope of the logarithmic section of the velocity profile is reflected by Reeves' formula [12] $\ell = \varkappa y\sqrt{\tau/\tau_w}$, the derivation of which was given in [7] with the difference that a binomial formula for τ was used in the transitional section. It should be noted that, in the present study, the coefficient κ_* is a parameter of the logarithmic velocity profile (3), not a proportionality factor in the formula for the mixing length $\ell = \varkappa y$. For a constant value of the coefficient κ equal to 0.4, the authors of [13] confirmed the advantages of the Reeves formula compared to the linear formula for mixing length. By using the Reeves formula with a constant value of κ in practical calculations, we essentially change over from the hypothesis of conservation of mixing length to the hypothesis of conservation of the slope of the logarithmic velocity profile. The curvilinear character of the change in ℓ corresponding to the Reeves formula was observed experimentally by E. M. Khabakhpashev and G. I. Efimenko [6] on the basis of very precise direct measurements of turbulent shear stress and experimental determination of $\partial u/\partial y$ in a boundary layer with a large positive pressure gradient.

Logarithmic Section of the Velocity Profile. The authors of [14] were the first to provide measurement data indicating a disruption of the conservativeness of the logarithmic section – of a contraction of the rectilinear segment of the logarithmic velocity profile at large positive pressure gradients. As was shown in [15], failure to allow for this contraction and the use of a logarithmic segment with constant values of κ_* and B_* to determine c_f (Clauser's method [10]) lead to underestimation of this quantity by 30-40% compared to data

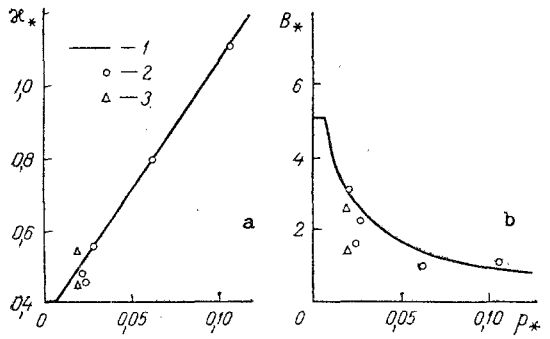

Fig. 1

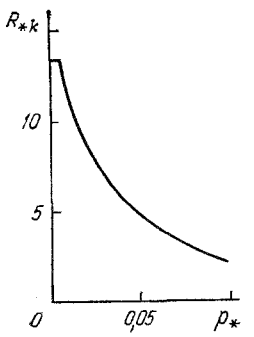

Fig. 2

Fig. 1. Dependence of the coefficients κ_*(a) and B_* (b) of the logarithmic velocity profile on the pressure gradient parameter: 1) by Eq. (4); 2) experimental data [4, 5]; 3) experimental data [6].

Fig. 2. Dependence of the critical local Reynolds number on the pressure gradient parameter.

from direct measurements. The studies [6, 16] made a more detailed investigation of the phenomenon of contraction of the rectilinear part of the logarithmic profile under the influence of a pressure gradient.

When the latest systematic measurements, taken within a broad range of the parameter p_* [4, 5], are replotted in the coordinates corresponding to wall law (1), it is found that an increase in the pressure gradient parameter p_* is accompanied not only by contraction of the rectilinear section of the logarithmic velocity profile (a decrease in B_*), but also by a decrease in the slope of this part relative to the x-axis (an increase in κ_*). Using these experimental findings together with experimental data from [6] to determine the functions $\kappa_*(p_*)$ and $B_*(p_*)$, we arrive at the relations shown in Fig. 1 together with the approximating functions:

$$\varkappa_* = \begin{cases} 0{,}4 & (p_* \leqslant 0{,}006), \\ 0{,}36 + 7{,}2\,p_* & (p_* > 0{,}006), \end{cases} \qquad B_* = \begin{cases} 5{,}1 & (p_* \leqslant 0{,}006), \\ 0{,}118\,(p_* + 0{,}017)^{-1} & (p_* > 0{,}006). \end{cases} \tag{4}$$

The latter formulas combine the law of conservation of the logarithmic section at small pressure gradients – established in [17] by direct measurements of shear stress on the wall – and the law of conservation of the form of logarithmic relation [4-6]. The coefficients of the rectilinear segment of the logarithmic velocity profile change from the values $\kappa_* = 0.4$ and $B_* = 5.1$ on the plate to $+\infty$ and 0 in the section corresponding to separation of the boundary layer. In this section, large-scale pulsative motion dominates the averaged motion and extends the zero velocity of the average motion from a point in the immediate vicinity of the wall to a certain finite region which is on the order of 1% of the thickness of the boundary layer. Thus, not only does the length of the logarithmic section decrease with approach toward the separation section [1, 2, 12], but the logarithmic dependence of longitudinal velocity on the transverse coordinate degenerates to an identically zero dependence.

By introducing the Reeves formula into the theoretical model – but with a variable coefficient κ_* [Eq. (4)] – we should be able to significantly improve the agreement of the calculated results with empirical data for large pressure gradients. It should be noted that, regardless of the quantity κ_*, use of the Reeves formula not only refines the formula for mixing length, but also entails a changeover from a direct method of calculation of the boundary layer to an inverse method – when a prescribed velocity profile is used to determine the shear stress distribution and mixing length.

Transitional Section of a Turbulent Boundary Layer in the Presence of a Large Positive Pressure Gradient. In the previous article [7], we determined the dependence of the damping factor on the transverse coordinate and the pressure gradient parameter. Calculations were performed with the assumption of the existence of a unique logarithmic section and constant values of the coefficients κ_* and B_* for different but small pressure gradients. Having repeated the analysis of the transitional section in [7] for variable values of κ_* and B_* with large pressure gradients, we find the function $R_{*k}(p_*)$ corresponding to these values (Fig. 2).

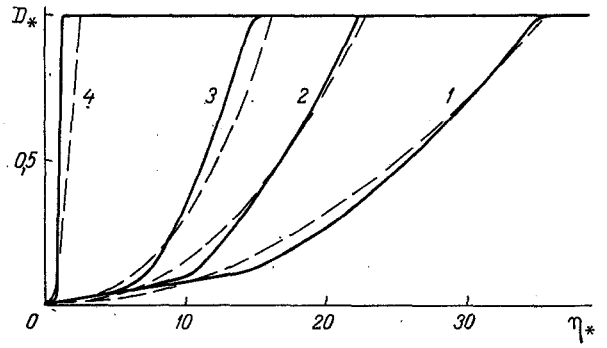

Fig. 3

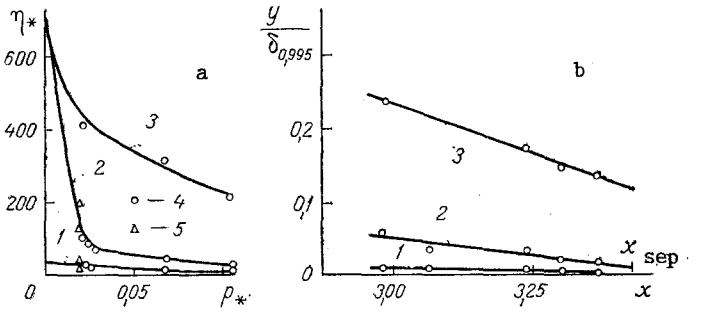

Fig. 4

Fig. 3. Family of curves of the damping factor corresponding to different values of the pressure gradient parameter (1) $p_* = 0$, 2) 0.01, 3) 0.02, 4) 0.1) obtained by numerical calculation (solid lines) and from an approximate formula (dashed lines).

Fig. 4. Structure of the velocity fields in the internal region of a turbulent boundary layer in the coordinates of the wall law (a) and in physical coordinates (b): 1) viscous sublayer and transitional section; 2) logarithmic section [for velocity – Eqs. (3) and (4)]; 3) section corresponding to half-power law [for velocity – Eqs. (6) and (7)] and the intermediate region; 4) experimental data on the boundaries between regions [4, 5]; 5) experimental data on the boundaries between regions [6]. x, m.

In a manner analogous to the classical longitudinal laminar-turbulent transition, the parameters R_{*k} – characterizing the ordinate of the point in the transitional section corresponding to the transition from viscous motion in the sublayer to turbulent motion in the core – decreases with an increase in the pressure gradient parameter p_* and takes a zero value in the separation section. The latter means that the transition begins in the immediate vicinity of the wall but does not lead to disappearance of the viscous sublayer – the region where laminar viscosity is considerably greater than eddy viscosity. It is evident from Fig. 3 that the thickness of the transitional section decreases with an increase in the pressure gradient parameter and vanishes in the separation section, where the damping factor D_* is equal to unity over the entire section and total viscosity is obtained simply by superimposing (without interaction) laminar and eddy viscosities. The dashed lines in Fig. 3 show an approximation of the curves of $D_*(\eta_*; p_*)$ by the piecewise-smooth family $D_{*a} = 0.0008 \times \exp(50p_*)(1 + p_*\eta_*)^2\eta_*^2$ $(\eta_* \leq \eta_{*0})$, $D_{*a} = 1(\eta_* > \eta_{*0})$, where η_{*0} is the coordinate at which the value of D_{*a} becomes equal to unity.

Structure of the Velocity Field in the Internal Region of the Turbulent Boundary Layer. At present, it is possible to completely understand the structure of the velocity field only in a nongradient boundary layer [1, 2]. Information on the change in this structure under the influence of a positive pressure gradient is extremely scarce and is only qualitative in character. Thus, in connection with the above-noted contraction of the straight section of the logarithmic profile, the authors of [4, 6, 14, 16] concluded that the thickness of the

viscous sublayer is decreased in the coordinates of wall law (1) compared to the nongradient case. It was indicated in [6, 12, 14, 16] that the size of the logarithmic section decreases sharply in the presence of a positive pressure gradient. Given this, the logarithmic law may be replaced by a half-power law [18]. In Stratford variables [7]

$$\eta_S = \frac{yv_S}{\nu}, \quad u_S = \frac{u}{v_S} \quad \left(v_S = \sqrt[3]{\frac{\nu}{\rho}\frac{dp}{dx}} \right) \tag{5}$$

the half-power law has the form

$$u_S = \frac{2}{\varkappa_S}\sqrt{\eta_S} + B_S. \tag{6}$$

An analysis of the experimental data in [4, 5] converted to the Stratford variables showed that, with a high degree of accuracy, the value of the coefficient $\varkappa_S$ turns out to be constant and equal to 0.6. Meanwhile, the coefficient B_S decreases with approach toward the separation section in accordance with the linear formula

$$B_S = 3{,}8\pi_S - 23{,}4. \tag{7}$$

Here, $\pi_S = (\nu/\rho(dp/dx))^{-2/3}v_*^2$ is the pressure gradient parameter written in Stratford variables [7]. Figure 4 shows the experimentally established boundaries between characteristic sections of the internal region: the transitional section, the logarithmic section, and the half-power-law section [4-6]. It can be seen from the figure that an increase in the pressure gradient parameter p_* is accompanied by a reduction in the total thickness of the viscous sublayer and the transitional section (as noted above, the thickness of the transitional section approaches zero going toward the separation section). We should point out that in the physical coordinates x and $y/\delta_{0.995}$, the configuration of the logarithmic section turns out to be wedge-shaped. The base of the wedge lies in the nongradient section, and there is a gradual contraction toward the separation section.

Continuing the analysis of experimental velocity profiles, we note that at moderate pressure gradients ($p_* \approx 0.01$) the logarithmic profile smoothly joins the half-power profile. In the case of large pressure gradients ($p_* \approx 0.1$), these profiles can no longer be joined by the derivative $\partial u/\partial y$, and an intermediate region is formed. The size of this region gradually increases with approach toward the separation section. The presence of this region can be judged from the appearance of two inflection points on the velocity profile, separated by a convex downward section. This feature is readily apparent against the background of convex upward graphs of the logarithmic and half-power velocity distributions. The thickness of the region corresponding to the half-power law in the nongradient section is equal to zero. At small pressure gradients, it increases with an increase in the parameter p_*. It then decreases as it approaches the separation section, so that the thickness of the entire internal region in this section is no greater than 5-7% of the thickness of the boundary layer.

NOTATION

x, y, longitudinal and transverse coordinates; u, longitudinal component of velocity; τ, total shear stress; τ_w, total shear stress on the wall; ρ, density; p, pressure; ν, viscosity coefficient; v_*, absolute viscosity; η, dimensionless transverse coordinate; p_*, π_S, pressure gradient parameters in the coordinates of the power law and the Stratford coordinates; g, parameter of convective acceleration; $\varkappa_*$, B_*, coefficients of the logarithmic velocity law; $\varkappa_S$, B_S, coefficients of the half-power law; $\varkappa$, proportionality factor in the formula for mixing length; c_f, friction coefficient on the wall; R_{*k}, critical local Reynolds number; D_*, damping factor; $\delta_{0.995}$, thickness of the boundary layer, i.e., distance from the wall to the point where the longitudinal component of velocity differs 0.5% from the velocity on the external boundary of the boundary layer; D_{*a}, coordinates of the point at which the damping factor D_{*a} becomes equal to unity; x_{sep}, coordinate of the boundary-layer separation point. The subscript * denotes variables of the wall law; S denotes Stratford variables (see [7]).

LITERATURE CITED

1. L. G. Loitsyanskii, Mechanics of Liquids and Gases [in Russian], Moscow (1987).
2. Yu. V. Lapin, Turbulent Boundary Layer in Supersonic Gas Flows [in Russian], Moscow (1982).

3. T. Cebeci, A. M. O. Smith, and G. Mosinskis, AIAA J., 8, No. 11, 1973-1982 (1977).
4. R. L. Simpson, Y. T. Chew, and B. G. Shivarprasad, J. Fluid Mech., 113, 23-51 (1981).
5. R. L. Simpson, J. Fluid Eng., 103, 520-533 (1981).
6. E. M. Khabakhpasheva and G. I. Efimenko, Structure of Forced and Thermogratitational Flows [in Russian], Novosibirsk (1983), pp. 5-31.
7. V. V. Zyabrikov and L. G. Loitsyanskii, Izv. Akad. Nauk SSSR, Mekh. Zhidk. Gaza, No. 5, 46-53 (1987).
8. D. Cowles, Boundary Layer Problems and Aspects of Heat Transfer [in Russian], Moscow, Leningrad (1960), pp. 138-147.
9. K. K. Fedyaevskii, A. S. Ginevskii, and A. V. Kolesnikov, Calculation of the Turbulent Boundary Layer of an Incompressible Fluid [in Russian], Leningrad (1973).
10. Proceed. Comp. of Turbulent Boundary Layer, AFOSR-I Fr., Stanford Conf. Themosciences Division, Dep. of Mech. Eng., California, USA, Vol. 2 (1969).
11. R. A. Galbraith and M. R. Head, Aeronaut. Q., 26, (pt. 2), 133-154 (1975).
12. B. L. Reeves, AIAA J., 12, No. 7, 932-939 (1974).
13. M. J. Nituch, S. Sjolander, and M. D. Head, Aeronaut. Q., 29, No. 3, 207-225 (1978).
14. G. I. Efimenko and E. M. Khabakhpasheva, Gradient and Separated Flows [in Russian], Novosibirsk (1976), pp. 49-68.
15. O. N. Kashinskii, S. S. Kutateladze, V. A. Mukhin, and V. E. Nakoryakov, Zh. Prikl. Mekh. Tekh. Fiz., No. 6, 92-96 (1974).
16. V. K. Lyakhov, M. I. Deveterikova, Yu. F. Ukrainskii, and S. Ya. Grabarnik, "Violation of the 'wall law' in flows with a positive pressure gradient," Submitted to VINITI 29.04.82, No. 2124-82 (1982).
17. H. Lidwieg and W. Tillman, Ing. Arch., 17, 288-299 (1949).
18. B. Ya. Kader and A. M. Yaglom, "Effect of roughness and a longitudinal pressure gradient on turbulent boundary layers," Itogi Nauki Tekh. Mekh. Zhidk. Gaza, 18, 3-111 (1984).

CALCULATION OF THE CHARACTERISTICS OF COUNTERCURRENT AXISYMMETRIC JETS

V. A. Dvoinishnikov, M. A. Laryushkin, and A. N. Rozhko

UDC 532.517.4

On the basis of analysis and generalization of experimental data, a method is proposed for calculating the parameters of the interaction of two coaxial jets flowing in opposite directions from circular nozzles of different diameters.

The operation of many types of equipment (boilers and dryers, high-pressure combustion chambers, etc.) is based on the interaction of countercurrent jets. In light of this, knowledge of the general laws governing their propagation acquires particular importance.

The literature data [1-3] shows that the propagation of a jet in an infinite opposing flow has been studied the most intensively, while there are almost no generalizing relations which describe the interaction of jets of finite dimensions.

We will examine the case of the coaxial interaction of two axisymmetric jets flowing in opposite directions from circular nozzles. The experiments were conducted on a unit with a fixed distance between the nozzles L_{ax} = 320 mm. The diameter of the large nozzle D was left constant and equal to 80 mm. The diameter of the small nozzle d was varied from 10 to 30 mm. Air was delivered to the system by a separate blower. The ratio of the impulses of the air jets $\bar{q} = \rho u^2/\rho_{\ell d} u_{\ell d}^2$ in the experiment was 0.2-4, which corresponded to a change in the Reynolds number $Re_{\ell d} = (4\text{-}2.5)\cdot 10^5$ for the large jet and $Re = (2\text{-}10)\cdot 10^4$ for the small jet.

Moscow Energy Institute. Translated from Inzhenerno-Fizicheskii Zhurnal, Vol. 56, No. 5, pp. 725-729, May, 1989. Original article submitted November 16, 1987.

 0022-0841/89/5605-0508$12.50